Malaysian Journal of Chemistry, 2026, Vol. 28(3), 141-150
(Special Issue: *International Conference on Chemistry and Sustainability, IC-CS 2025*)

Graphene–Yb_2O_3 Nanocomposites for Enhanced Photocatalytic and Electrochemical Properties using Data-Driven Analysis

Kusum[1], Nitu Sehrawat[2] and Srishti Vashishtha[3]*
[1]Research Scholar, Department of Chemistry, Baba Mastnath University, Rohtak, Haryana, India
[2]Applied Science Department, Bharati Vidyapeeth's College of Engineering, New Delhi –110063 (India)
[3]Department of Computer Science and Engineering, Bharati Vidyapeeth's College of Engineering, New Delhi - 110063, (India)
*Corresponding author (e-mail: srishtidtu@gmail.com)

A Nanocomposites of graphene and ytterbium oxide were created through the amalgamation of graphene oxide and Yb2O3 in different weight proportions (Yb2O3G1, Yb2O3G3, Yb2O3G5). The materials were analysed through a multitude of sophisticated methods such as X-ray diffraction (XRD), Raman spectroscopy, Fourier-transform infrared spectroscopy (FTIR), scanning electron microscopy (SEM), transmission electron microscopy (TEM), energy dispersive spectroscopy (EDS), "X-ray photoelectron spectroscopy (XPS), and electrochemical assessments." Analyses of the structure revealed that graphene had a negligible effect on the crystallinity of Yb2O3, accompanied by slight alterations in the diffraction peaks. The successful creation of Yb2O3-graphene composites was validated through Raman and FTIR spectra analysis. The morphological investigations unveiled a notable improvement in the distribution of Yb2O3 crystals throughout the graphene matrix, particularly at elevated concentrations of graphene. The examination of electrochemical characteristics revealed that the impact of graphene on the electrochemical attributes of Yb2O3 was minimal, whereas the performance in photocatalysis saw a notable enhancement. The Yb2O3G5 composite demonstrated exceptional photocatalytic performance in breaking down methylene blue (MB) dye when exposed to UV light, underscoring the promising capabilities of these composites for environmental remediation efforts.

Keywords: Graphene-Yb_2O_3 nanocomposites, photocatalysis, energy storage, dye degradation, environmental cleanup

Received: March 2026; Accepted: April 2026

As observed in the earlier sections, rare earth oxide nanomaterials have been thoroughly examined and recognized as promising substances for optoelectronic applications, photoluminescent properties, photocatalytic functions, and also in medical uses. Materials derived from carbon, including activated carbon, porous carbon, and carbon nanotubes, have been extensively examined for their appropriateness in this context. The pinnacle of innovation, a singular atom thick flat layer of sp2 linked carbon atoms; graphene has sparked a transformation in contemporary materials science and technological advancements. Composite materials derived from metal oxides and graphene have garnered significant interest lately due to their enhanced storage capacity, remarkable cyclic stability, and impressive photocatalytic characteristics. Nonetheless, it is recognized that the uncommon earth oxide infused graphene composites have been infrequently examined for their electrochemical characteristics.

Building upon the preceding chapter, this section discusses the preparation of graphene Yb2O3 nanocomposites utilizing various weight ratios of graphene combined with Yb2O3. The composite substances were examined through a range of analytical methods. Nonetheless, enhanced photocatalytic efficacy was noted for the composite featuring a greater proportion of graphene. Consequently, this study emphasizes Yb2O3G nanocomposite as a pivotal component for energy storage and photocatalytic applications.

SYNTHESIS OF GRAPHENE-Yb2O3 COMPOSITE

For the creation of Ytterbium oxide-graphene (Yb2O3G) composites, 99 mg of commercially acquired yttrium oxide (99.9%) was thoroughly mixed in 100 ml of water using ultra-sonication, followed by the incorporation of 1 mg of synthesised graphene into the mixture [1]. The mixture was kept at ambient temperature while being continuously stirred for a duration of 2 hours. The ultimate outcome Yb2O3G1 was gathered and dehydrated in a vacuum at 60°C for a duration of 24 hours. Using the identical method, Yb2O3G3 and Yb2O3G5 composites were synthesised by incorporating

†Paper presented at the International Conference on Chemistry and Sustainability, IC-CS 2025

97 mg of Yb2O3 along with 3 mg of graphene and 95 mg of Yb2O3 combined with 5 mg of graphene, correspondingly. The impact of graphene on the structural, electrochemical, and photocatalytic characteristics of ytterbium oxide has been examined through diverse methodologies. The operational characteristics such as cyclic voltammetric response and photocatalytic efficiency were examined using appropriate techniques [2].

CHARACTERIZATION TECHNIQUES

The synthesised nanocomposites underwent characterisation through a range of analytical methodologies. The Rigaku MiniFlexII-C X-ray diffractometer utilised CuKĮ (O = 1.540 nm) radiation at a scanning velocity of 1 deg/min to gather the powder X-ray diffraction information for material identification. Raman and FTIR spectra were obtained to validate the creation of composites using the JASCO Raman Spectrophotometer (NRS – 7100) and the NICOLET Infrared spectrophotometer, respectively [3]. The structure of the composites underwent examination through FE-SEM and HR-TEM imagery acquired via JEOL 7001F and JEOL-JEM 2100F electron microscopes, correspondingly. The fundamental makeup was examined through elemental mapping and EDS spectra acquired using the JEOL JXA 8530F model Field Emission Electron Probe Micro Analyser (FE-EPMA) device. The binding energies of electrons for different elements within the composites were examined using the ESCA 3400 SHIMADZU X-ray photo-electron spectrometer [4]. The electrochemical behaviour of the composites was examined through a three-electrode setup utilising a Bio Logic electrochemical workstation. Glassy carbon, Ag/AgCl, and platinum wire have been utilised as the working, reference, and counter electrodes, respectively. The cyclic voltammetric profiles were captured within the spectrum from -0.3 to 0.6 at scanning velocities of 5, 10, 15, 25, 50, and 100 mV/s employing 1 M H2SO4 as the electrolyte solution. The photocatalytic efficacy of the nanocomposites was examined by documenting absorption variations of dye molecules through a (CARY 500) Scan UV–Vis-NIR spectrophotometer.

RESULTS AND DISCUSSION

Powder X-ray Diffraction Studies

X-ray diffraction patterns of the synthesised graphene, pristine ytterbium oxide, and Yb2O3G nanocomposites were captured, as illustrated in Figure 2.1(a-e). The diffraction pattern exhibited by graphene reveals solely two peaks that align with the 002 and 100 diffraction planes, as illustrated in Figure 1 (e). Conversely, the diffraction patterns observed for ytterbium oxide and its composites exhibit a significant number of pronounced peaks, which guarantees a robust crystalline structure, as illustrated in Figure 1(a-d). The diffraction patterns are analysed in relation to the reference JCPDS # 65-3173 for cubic ytterbium oxide, and the peaks were indexed correspondingly [6]. Based on the observed patterns, it is evident that the impact of graphene is minimal due to the substantial amount of ytterbium oxide present. Upon meticulous scrutiny of the amplified peaks at diverse two theta values, it was noted that the existence of graphene has subtly displaced the peaks towards the diminished diffraction angle and diminished the peak intensity (Figure 2a & b). The detected peak displacement arises from the lattice deformation existing in the Yb2O3G composites [7].

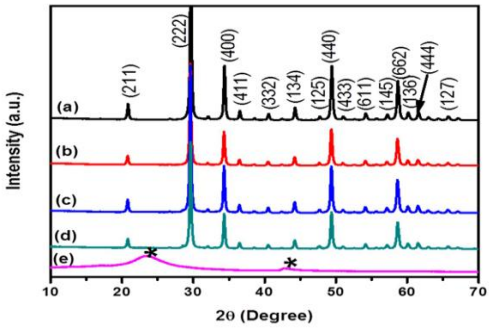

Figure 1. Powder X-ray diffraction pattern of (a) pure Yb2O3, (b) Yb2O3G1, (c) Yb2O3G3, (d) Yb2O3G5 composites and (e) synthesized graphene.

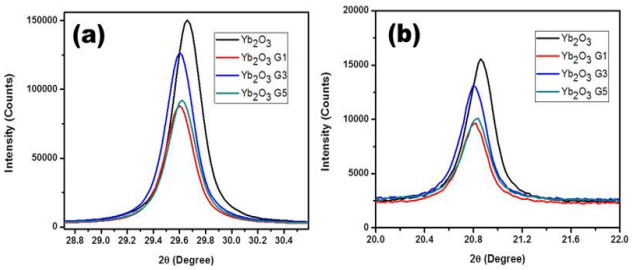

Figure 2. Powder X-ray diffraction plane of (a) (222) and (b) (211) shows the mild peak shift towards lower angle.

Laser Raman Spectral Studies

Laser Raman spectra were captured for the graphene, Yb2O3, Yb2O3G1, and Yb2O3G5 composites within the wavenumber range of 100 to 2000 cm-1. The range of pristine graphene exhibits no peaks between 100 and 800 cm-1 (refer to Figure 3a), while the distinctive peaks known as D and G bands appear at 1343 and 1580 cm-1, respectively, as illustrated in Figure 3b. The intensity ratio of the D and G bands, ID/IG, for graphene is recorded as exceeding 1 (1.11). Consequently, the graphene derived from GO exhibits an organised structure and possesses commendable quality, ensuring the presence of sp2 bonded carbon. Conversely, the Yb2O3G1 and Yb2O3G5 composites exhibit a greater quantity of peaks within the range of 100 to 800 cm-1, alongside the D and G bands of graphene found in the spectrum of 800 to 2000 cm-1 [8]. The bands have remained largely unchanged; nonetheless, the intensity ratio between the D and G bands has decreased from 1.11 to 1.016 with the rising quantity of graphene. The diminished intensity ratio and an increased count of peaks serve as proof for the creation of the Yb2O3G5 composite. The extra peaks observed at 455 cm-1 with increased intensity result from the composite [9].

FTIR Spectral Studies

FTIR spectral analyses have revealed the existence of functional groups within Yb2O3G composites. The spectra have been captured within the wavenumber spectrum spanning from 400 to 4000 cm-1, as illustrated in Figure 3. The spectra reveal that the band near 3500 cm-1 corresponds to the absorbed moisture from the environment, which is significantly less intense in the composites than in pure Yb2O3 [10]. Typically, the stretching vibrations of carbon dioxide are found within the range of 3000 to 1000 cm-1, which manifest in the pristine Yb2O3 FTIR spectrum as a result of atmospheric carbon dioxide's presence. The bands were diminished in the composites, and the absorption peak observed at 584 cm-1 corresponds to the stretching vibrations of Yb-O, which exhibited a reduction in intensity in the Yb2O3G5 sample. The subtle oscillations associated with carbon and oxygen detected in the composites validate the creation of Yb2O3G composites [11].

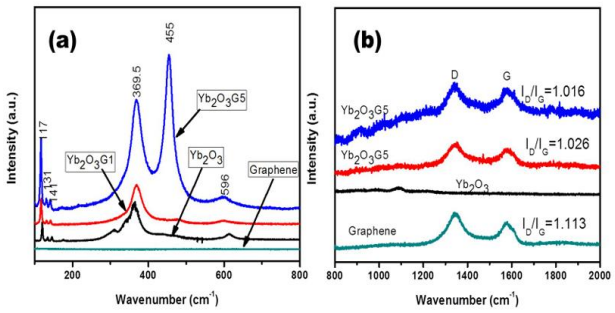

Figure 3. Raman spectra of graphene and Yb2O3G nanocomposites at region between (a) 100-800 cm^{-1} and (b) 800-2000 cm^{-1}

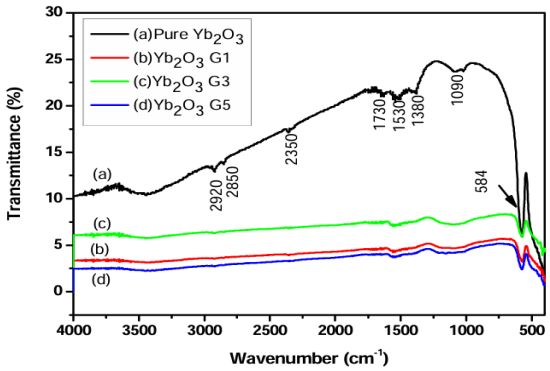

Figure 4. FTIR spectra of (a) Pure Yb2O3, (b) Yb2O3G1, (c) Yb2O3G3 and (d) Yb2O3G5 nanocomposites.

Morphological Analysis

The structure of the acquired pure Yb2O3 and composites was examined using FE-SEM, with the resulting images displayed in Figures 5 and 6, respectively. The structure of unadulterated Yb2O3 comprises microcrystals exhibiting an uneven form, as illustrated in Figure 5(a). The enlarged depiction (Figure 5(b)) confirmed that Yb2O3 comprises both nano and microcrystals. The structure of the composite Yb2O3G1 features graphene layers interspersed among Yb2O3 crystals, as illustrated in Figure 5(a) [12]. The enlarged depiction (Figure 5(b)) confirmed that the Yb2O3 Crystals were enveloped by the graphene, thus resulting in the formation of the composites. The tiny visuals of Yb2O3G5 composite (Figure 6c & 6d) suggested that a significant quantity of Ytterbium oxide crystals contributed to the creation of the composite, and the enlarged image confirmed that the flake-like structure of the composite has been established.

The rise in the weight percentage of graphene has led to the clustering of Yb2O3 alongside graphene, resulting in a distorted, flake-like configuration of the graphene structure, as illustrated in Figure 6d. Moreover, it is evident from the calibre of the visuals that the graphene layers have been successfully diminished from GO [13].

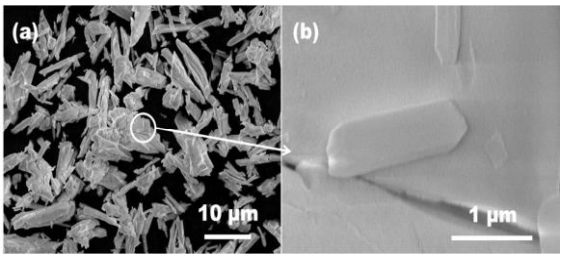

Figure 5. FE-SEM images of Pure Yb2O3 at different magnifications.

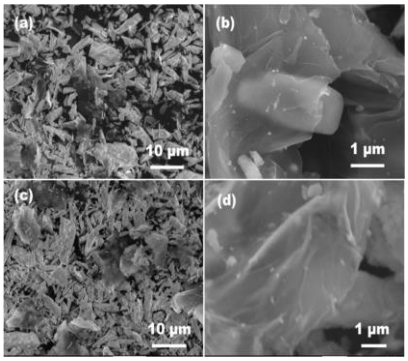

Figure 6. FE-SEM images of (a, b) Yb2O3G1 and (c, d) Yb2O3G5 at different magnifications.

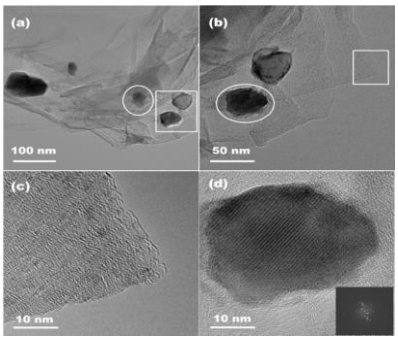

Figure 7. HR-TEM images of YbOG5 nanocomposite from lower to higher magnification.

High-resolution transmission electron microscopy images of Yb2O3G5 at various magnifications are presented in Figure 7 (a-d). The illustration reveals that the Yb2O3 crystals are situated amidst the graphene sheets, specifically in the highlighted area of Figure 6a. The enlarged depiction suggests that the dimensions of the crystals are below 100 nm, as illustrated in Figure 6b [14]. The images with elevated magnification of the designated area in Figure 7b are presented in Figures 7c and 7d. A slender collection of graphene layers as a segment of the composite has been distinctly noted, and the Yb2O3 crystal identified within the nanocomposite exhibits a pronounced crystalline quality. The image distinctly reveals lattice fringes, confirming the crystalline characteristics. The FFT pattern that aligns with Figure 7d is displayed in the inset [15].

Table 1. Measured elemental composition of reduced graphene and Yb2O3G composites.

Sample	Element	Atomic %	Error
Graphene	C K	85.67	0.12
	O K	14.33	1.23
Yb_2O_3	Yb L	397	0.79
	O K	63.03	0.29
Sulfur	Yb L	7.92	0.58
	C K	69.79	0.09
Yb_2O_3G1	O K	22.30	0.28
	Yb L	4.90	0.56
Yb_2O_3G5	C K	75.88	0.08
	O K	19.22	0.30

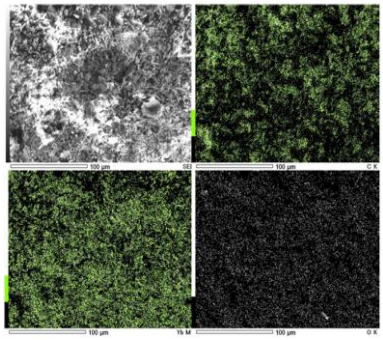

Figure 8. FE-EPMA images of Yb_2O_3G5.

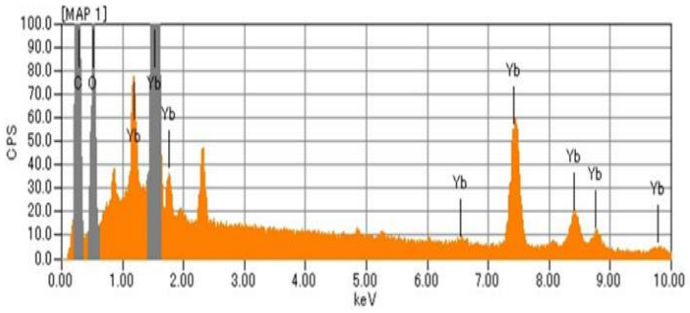

Figure 9. Energy dispersive spectrum of Yb_2O_3G5.

Elemental Analysis

The crafted composites underwent electron probe microanalysis, and the elemental mapping was documented. The FE-EPMA mapping demonstrates that the levels of ytterbium and carbon are markedly elevated compared to those of oxygen, as illustrated in Figure 8. The energy dispersive spectrum associated with the Yb2O3G5 composite is illustrated in Figure 9. The fundamental makeup of carbon, oxygen, and ytterbium elements was assessed for Yb2O3, Yb2O3G1, and Yb2O3G5 composites, and the findings were organised in Table 1 [16]. The mole percentage of ytterbium in the chosen area of the composite has shown a decline as the carbon concentration has risen.

X-ray Photoelectron Spectral Analysis

The survey range of Yb2O3G5 composite has been captured using an X-ray photoelectron spectrometer, as illustrated in Figure 10. It possesses auditory indicators for oxygen and carbon 1s electrons; however, the indicator for ytterbium 4d electrons remained unrecognised in the survey spectrum. Consequently, the fundamental core level XPS spectra of diverse elements for the Yb2O3G5 composite have been acquired. The fundamental spectrum of 4d ytterbium within the range of 170-210 eV is illustrated in Figure 11. This features solely a singular summit at 183 eV [17]. The fundamental XPS spectrum for C 1s is illustrated in Figure 12, featuring two distinct peaks at 285.1 and 288.9 eV, attributed to sp2 hybridised carbon (C-C) and carboxyl groups (C-O), correspondingly. This suggests that carbon possesses a substantial quantity of oxygen-rich functional groups that can boost photocatalysis by capturing the photoinduced holes (Chen et al 2012), thereby amplifying the generation of potent oxidising OH radicals (Xu et al 2008). Distinct oxygen species can be identified by examining the O1s spectrum within the energy range of 525 to 540 eV, as illustrated in Figure 3.13. The binding energies of 530.8 eV and 532.6 eV have been attributed to lattice oxygen and hydroxyl groups, correspondingly (Chen et al 2012).

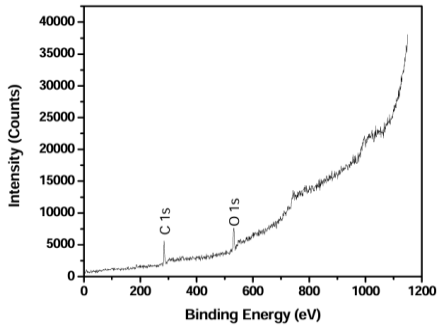

Figure 10. X-ray photoelectron survey spectrum of Yb2O3G5.

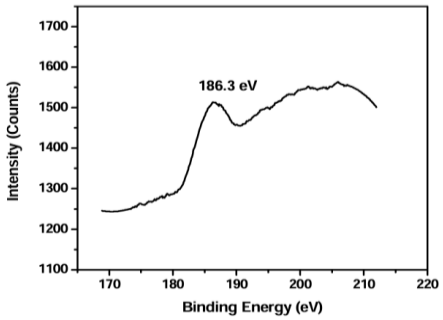

Figure 11. Core level X-ray photoelectron spectra of ytterbium4d electron in the Yb2O3G5 Composite.

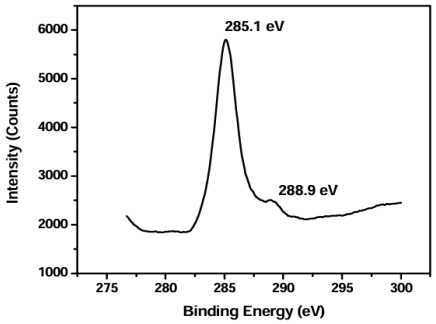

Figure 12. Core level X-ray photoelectron spectra of carbon 1s electron in the Yb2O3G5 Composite.

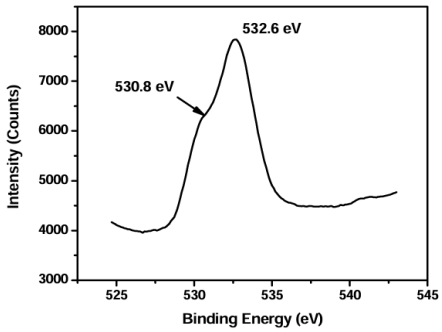

Figure 13. Core level X-ray photoelectron spectra of oxygen 1s electron in the Yb2O3G5 Composite.

Cyclic Voltammetric Behavior

Cyclic Voltammetric assessments of Yb2O3G nanocomposites were conducted in a water-based solution of 1M H2SO4, utilising a potential span from -0.2 to 1 V. The voltammogram obtained for Yb2O3G5 at various scanning rates is illustrated in Figure 14 [18]. The redox characteristics of metal oxides were noted, and an asymmetric change was detected at scanning rates beneath 15 mV/s. Nevertheless, surpassing a scan rate of 25 mV/s, almost square, seamless cyclic voltammetry loops were noted, exhibiting gentle redox activity similar to earlier instances. The present and overall region of the CV loop has expanded with an elevation in the scan rate, signifying the favourable capacitance characteristics of nanocomposites [19].

The precise capacitance measurements for Yb2O3G5 have been determined from the area of the CV curve utilising Equation (1).

$$Cs = {}^{3}IdV/vmV. \quad (1)$$

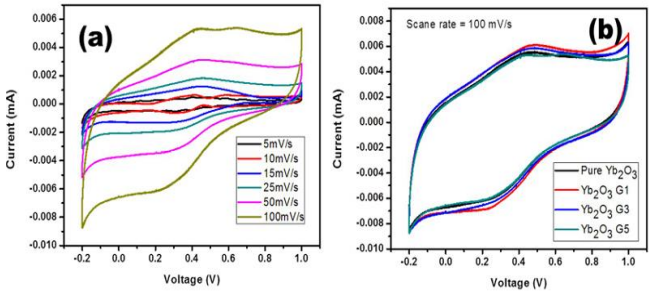

Figure 14. (a) cyclic voltommogram for Yb2O3G5 nanocomposite at different scan rate and (b) Comparison of CV loop of pure Yb2O3, Yb2O3G1, Yb2O3G3 and Yb2O3G5.

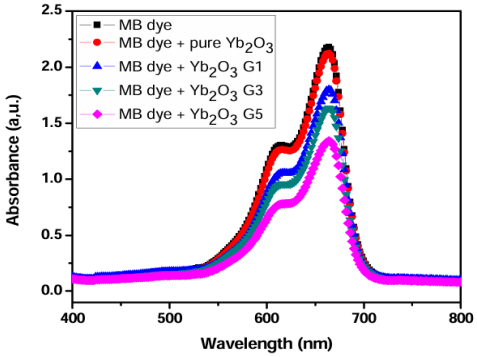

Figure 15. Absorption spectra of MB dye, MB dye with Yb2O3 and MB dye with Yb2O3G nanocomposites after the solution is irradiated by UV light for 30 minutes.

In this context, I represents the response current, V denotes the potential, v indicates the potential scan rate, and m refers to the mass of the active material present on the electrode. The specific capacitance values for Yb2O3G5 nano composite were measured, revealing a decline as the scan rate increased. The CV assessments for Yb2O3, Yb2O3G1, and Yb2O3G3 were similarly performed under identical conditions. The outcomes were nearly identical and revealed no notable improvement attributed to the existence of graphene. The findings clearly indicate that the impact of graphene on the electrochemical characteristics of Yb2O3 is minimal, attributed to the inadequate quantity of graphene incorporated in this study. Nonetheless, it is observed that the inclusion of graphene has not diminished the capacitive characteristics of the Yb2O3.

Photocatalytic Property

The photocatalytic performance of the synthesised composites for dye breakdown was evaluated using MB dye under UV light exposure, and the findings are illustrated in Figure 15. The experiment on dye degradation was conducted for both pure Yb2O3 and Yb2O3G composites during an identical duration of UV light exposure. The liquid mixtures of MB dye combined with pristine Yb2O3 and Yb2O3G nanocomposites underwent exposure to UV radiation for a duration of 30 minutes, during which the changes in the distinctive absorption peaks of MB dye at 662 nm and an additional shoulder peak at 610 nm were meticulously examined [20]. The illustration indicates that the proportion of graphene within the composite markedly affected the dye degradation performance, revealing that Yb2O3G5 exhibits superior catalytic efficiency compared to other Yb2O3G composites and pure Yb2O3. It has been noted that 40% of the dye has undergone degradation within a few minutes of exposure to UV radiation in the dye solution containing Yb2O3G5 composite. Nonetheless, identical observations have been noted at 25, 17, and 3% correspondingly for the dye solutions comprising Yb2O3G3, Yb2O3G1 composites, and Yb2O3.

The process of photo degradation primarily relies on the creation of photo-induced charge carriers (electron-hole pairs), the separation of charges, and their movement to the surface. On the surfaces, surface hydroxyl captures the electrons and holes, resulting in the formation of hydroxyl radicals. Yb2O3 serves as an excellent photocatalytic substance owing to its elevated valence band (VB) potential, leading

to the generation of holes possessing substantial oxidative capacity, thereby enabling the oxidation of OH- into OH radicals. Conversely, the absorption of dye would surpass that observed in the unadulterated Y2O3, attributed to the elevated surface area of graphene. Furthermore, the oxygen levels are minimal in the synthesised reduced graphene, as verified by EPMA analysis (Table 1). Consequently, the oxygen reaction sites, such as C-O groups, are restricted in the nanocomposite with diminished graphene content (Yb2O3G1 and Yb2O3G3) [21]. The elevated dye uptake and the diminished oxygen levels result in reduced photocatalytic performance in the specimens Yb2O3G1 and Yb2O3G3. With an elevated mole percentage of graphene (Yb2O3G5), the reaction sites for oxygen are augmented owing to the substantial quantity of graphene present in the composite. Furthermore, the levels of oxide and hydroxyl radicals were elevated in the samples, leading to enhanced photocatalytic efficacy. Furthermore, the Yb2O3-graphene nanocomposite hinders the recombination of excitons, resulting in effective charge separation. The XPS analysis indicates that the existence of hydroxyl groups and surface oxygen within the nanocomposite enhances the formation of OH and oxygen radicals. The creation of these radicals leads to the breakdown of dye molecules.

CONCLUSION

In this study, graphene-Yb2O3 nanocomposites were successfully synthesized and their structural, electrochemical, and photocatalytic properties were thoroughly investigated. The results show that the addition of graphene significantly enhances the photocatalytic performance of Yb2O3, particularly in the Yb2O3G5 composite, which exhibited improved dye degradation efficiency. Electrochemical measurements also revealed favorable capacitance characteristics in the composites, suggesting potential applications in energy storage. The synergy between graphene and Yb2O3 led to an efficient charge separation and enhanced photocatalytic properties. These findings highlight the potential of graphene-infused Yb2O3 composites for advanced energy and environmental applications, particularly in photocatalysis and energy storage devices.

REFERENCES

1. Hu, C., Lu, T., Chen, F. and Zhang, R. (2013) A brief review of graphene–metal oxide composites synthesis and applications in photocatalysis. *Journal of the Chinese Advanced Materials Society*, **1(1)**, 21–39.

2. Potbhare, A. K., Aziz, S. T., Ayyub, M. M., Kahate, A., Madankar, R., Wankar, S., Dutta, A., Abdala, A., Mohmood, S. H., Adhikari, R. and Chaudhary, R. G. (2024) Bioinspired graphene-based metal oxide nanocomposites for photocatalytic and electrochemical performances: an updated review. *Nanoscale Advances*, **6(10)**, 2539–2568.

3. Olatunde, O. C. & Onwudiwe, D. C. (2022) A comparative study of graphene oxide/graphitic carbon nitride composites in photocatalysis. *Catalysts*, **12(1)**, 14. https://doi.org/10.3390/catal12010014.

4. Kumar, S., Chaudhary, G. R. & Chaudhary, S. (2022) Designing of surface engineered Ytterbium oxide nanoparticles as effective electrochemical sensing platform for dopamine. *Journal of Molecular Liquids*, **355**, 118929.

5. Al-Rawashdeh, N. A., Allabadi, O. & Aljarrah, M. T. (2020) Photocatalytic activity of graphene oxide/zinc oxide nanocomposites with embedded metal nanoparticles for the degradation of organic dyes. *ACS omega*, **5(43)**, 28046–28055.

6. Mandal, S., Mallapur, S., Reddy, M., Singh, J. K., Lee, D. E. & Park, T. (2020) An overview on graphene-metal oxide semiconductor nano-composite: A promising platform for visible light photocatalytic activity for the treatment of various pollutants in aqueous medium. *Molecules*, **25(22)**, 5380.

7. Saravanan, T., Anandan, P., Shanmugam, M., Azhagurajan, M., Mohamed Ismail, M., Arivanandhan, M. & Jayavel, R. (2020) Facile synthesis of Yb2O3–graphene nanocomposites for enhanced energy and environmental applications. *Polymer Bulletin*, **77(8)**, 3891–3906.

8. Hoseynidokht, F., Mazloum-Ardakani, M. & Farbod, F. (2025) Novel electrochemical immune-sensor enhanced with ytterbium oxide nano-particles integrated into nitrogen-doped graphene aerogel for detection of aquaporin-4 autoanti-bodies. *Microchemical Journal*, 116476.

9. Mushahary, N., Sarkar, A., Basumatary, F., Brahma, S., Das, B. & Basumatary, S. (2024) Recent developments on graphene oxide and its composite materials: From fundamentals to applications in biodiesel synthesis, adsorption, photocatalysis, supercapacitors, sensors and antimicrobial activity. *Results in Surfaces and Interfaces*, **15**, 100225.

10. Som, T., Troppenz, G. V., Wendt, R., Wollgarten, M., Rappich, J., Emmerling, F. & Rademann, K. (2014) Graphene Oxide/α-Bi2O3 Composites for Visible-Light Photocatalysis, Chemical Catalysis, and Solar Energy Conversion. *ChemSusChem*, **7(3)**, 854–865.

11. Zhang, F., Liu, J., Hu, L. & Guo, C. (2024) Recent progress of three-dimensional graphene-based composites for photocatalysis. *Gels*, **10(10)**, 626.

12. Jamjoum, H. A. A., Umar, K., Adnan, R., Razali, M. R. & Mohamad Ibrahim, M. N. (2021) Synthesis, characterization, and photocatalytic activities of graphene oxide/metal oxides nanocomposites: A review. *Frontiers in Chemistry*, **9**, 752276.

13. Upadhyay, R. K., Soin, N. & Roy, S. S. (2014) Role of graphene/metal oxide composites as photocatalysts, adsorbents and disinfectants in water treatment: a review. *RSC Advances*, **4(8)**, 3823–3851.

14. Chang, H. & Wu, H. (2013) Graphene-based nanocomposites: preparation, functionalization, and energy and environmental applications. *Energy & Environmental Science*, **6(12)**, 3483–3507.

15. Baby, A., VP, A. & Balakrishnan, S. P. (2025) Graphene–Metal Oxide Composites for Electrochemical Energy Storage and Conversion.

16. Lee, Y. & Kim, S. (2020) Enhanced photocatalytic degradation using reduced graphene oxide/TiO_2 nanocomposites. *Chemical Engineering Journal*.

17. Pavitra, V., Soni, I., Praveen, B. M. & Nagaraju, G. (2023) Brief review on carbon derivatives based ternary metal oxide composite electrode materials for lithium-ion batteries. *Journal of Electrochemical Science and Engineering*, **13(4)**, 605–640.

18. Deng, S., Sun, D., Wu, C., Wang, H., Liu, J., Sun, Y. & Yan, H. (2013) Synthesis and electrochemical properties of MnO2 nanorods/graphene composites for supercapacitor applications. *Electrochimica Acta*, **111**, 707–712.

19. Zhao, H., Wang, Q. & Zhang, Y. (2022) Recent advances in graphene oxide composites for photocatalysis. *Journal of Materials Science*, **57(5)**, 3334–3347. https://doi.org/10.1007/s10853022 068691.

20. Smith, A. (2018) Charge transfer mechanisms in graphene metal oxide hybrid photocatalysts. *Applied Surface Science (Broad field study)*.

21. Tan, S. Y., Chong, W. C., Sethupathi, S., Pang, Y. L., Sim, L. C. & Mahmoudi, E. (2023) Optimisation of aqueous phase low density polyethylene degradation by graphene oxide-zinc oxide photocatalysts. *Chemical Engineering Research and Design*, **190**, 550–565.